16th World Conference on Earthquake, 16WCEE 2017

Santiago Chile, January 9th to 13th 2017

Paper N° 690

Registration Code: S-V1461828123

STRUCTURAL PERFORMANCE OF DAMAGED OPEN-WEB TYPE SRC BEAM-COLUMNS WITH BOLT-CONNECTED BATTEN STEEL PLATES AFTER RETROFITTING

T. Fujinaga[(1)], Y. Sun[(2)]

[(1)] *Associate Professor, Research Center for Urban Safety and Security, Kobe University, ftaka@kobe-u.ac.jp*
[(2)] *Professor, Faculty of Engineering, Kobe University, sunlili@people.kobe-u.ac.jp*

The structural performance of damaged open-web type of steel encased reinforced concrete (SRC) beam-columns with bolt-connected batten steel plates after retrofitting was experimentally investigated. The experimental parameters are axial load ratio, shear span ratio, and the maximum tip displacement of the columns during the initial loading. First, each column was cyclically loaded to the targeted displacement. Subsequently, the test columns were retrofitted and reloaded. The damaged portions of each column were retrofitted with the polymer cement mortar, and the epoxy resin was injected into the cracks.

Experimental results indicated that the measured stiffness of retrofitted columns was lower than the initial ones while the experienced displacements in each column were different. The lower stiffness might be attributed to deterioration of the concrete rigidity, low rigidity of the resin, and imperfect injection of the resin. Test results also indicate the column which experienced the larger displacement and higher axial load showed lower load carrying capacity, but the others showed approximately equal capacities to those of the initial columns. The lower load carrying capacity of the column resulted from buckling of the longitudinal reinforcements.

The crack width was measured to assess the relation of crack width and the experienced drift ratio. These are valuable to predict the degree of damage from the crack width after an earthquake.

Numerical analyses were also conducted to explain the retrofitted column behavior. The effect of strain hysteresis of concrete at first loading was considered for the behavior at second loading. Results predicted the experimental behaviors fairly well, which implies the validity of the analytical methods presented in this paper for evaluating the structural performance of retrofitted SRC columns in low axial load.

Keywords: Cracks, Stiffness, Load carrying capacity, Epoxy resin, Polymer cement mortar

1. Introduction

After a strong earthquake, many damaged buildings are demolished and reconstructed instead of being seismically retrofitted and reused, even though many of them are only damaged moderately, because the structural performance of damaged buildings after retrofitting is unclear, which makes it difficult to evaluate the degree of recovery of structural performance of the damaged components and structures accurately [Report on Hanshin-Awaji EQ 1998].

Recently, we obtained fundamental data related to the seismic recovery of damaged reinforced concrete (RC) beam-columns and damaged open-web-type steel-encased reinforced concrete (SRC) beam-columns with weld-connected batten and lattice steel plates after retrofitting [Fujinaga and Sun 2010]. However, the batten steel plates of open-web type SRC beam-columns, sustained considerable damage during the Kobe earthquake, were almost bolt-connected or rivet-connected ones. As described herein, open-web type SRC beam-column specimens with bolt-connected batten steel plates encasements were fabricated and tested under combined constant axial load and cyclic lateral loads. The objectives of this paper are 1) to elucidate the structural performance of damaged open-web type SRC beam-columns and 2) to evaluate, both experimentally and analytically, the structural performance of retrofitted beam-columns.

2. Experiment of open-web type SRC beam-columns

2.1 Outline of experiment

Test specimens were open-web type SRC beam-columns and their encasements built with bolt-connected batten steel plates. Specimens were tested under combined constant axial load and cyclic lateral load, using the loading apparatus shown in Figure 1. First, each beam-column was loaded cyclically to a targeted displacement. After the first loading, the specimens were retrofitted and reloaded. Damaged portions of each column were retrofitted with polymer cement mortar. Then epoxy resin was injected into the cracks.

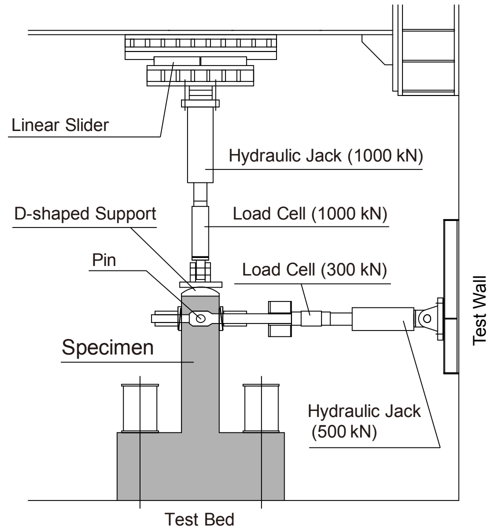

Fig. 1 – Loading apparatus.

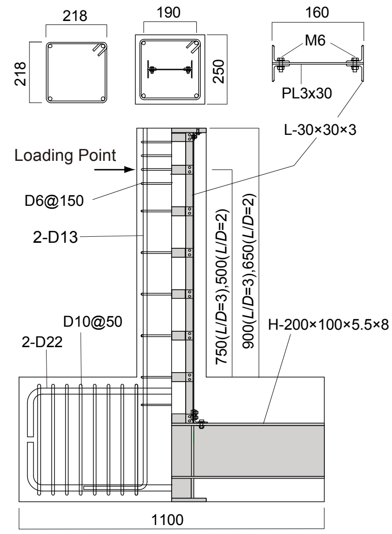

Fig. 2 – Test specimen (mm).

Table 1 – Test conditions

Specimens		Shear span ratio	Axial load ratio $n=N/N_0$*	Maximum rotation angle (rad)	Method of Retrofitting	Young's Modulus of Concrete ${}_cE$ ($\times 10^3$ N/mm^2)	Comp. Strength of Concrete F_c (N/mm^2)	Tens. Strength of Concrete F_t (N/mm^2)
1st loading	B3-B2	3	0.2	0.03	-	21.6	24.5	2.50
	B3-B4		0.4	0.02	-	23.8	24.1	2.43
	B3-M4			0.015	-	22.7	24.3	2.46
2nd Loading	B3-B2-R		0.2	-	Section repair Injection of epoxy	23.8 10.2^{**}	26.3 20.1^{**}	2.11 2.67^{**}
	B3-B4-R		0.4	-		22.8 10.1^{**}	25.0 21.2^{**}	2.36 2.53^{**}
	B3-M4-R			-		21.8 8.83^{**}	24.5 20.6^{**}	2.00 1.93^{**}
1st loading	B2-M2	2	0.2	0.02	-	25.0	27.3	2.59
	B2-B4		0.36	0.02	-	18.1	17.3	1.80
	B2-M4			0.01	-	17.7	17.9	1.82
2nd Loading	B2-M2-R		0.2	-	Injection of epoxy	22.6	28.8	2.49
	B2-B4-R		0.36	-	Section repair Injection of epoxy	18.5 12.1^{**}	15.9 19.0^{**}	0.65 2.20^{**}
	B2-M4-R			-	Injection of epoxy	17.3	16.3	1.73

* $N_0 = {}_cA\,F_c + {}_sA\,{}_sY$, ** Polymer cement mortar

2.2 Specimen

Six specimens were fabricated and tested (see Figure 2). The section width and depth were 250 mm. It had a loading block for fixing to the test bed. The steel encasement was open web type. It was built with chord angles (L-30×30×3) and batten steel plates (32×3 mm) and was connected with bolts. The steel encasement depth was 160 mm, with batten plate spacing of 150 mm. The bolts are M6. The introduced torque was 15 kNm. Main reinforcements are steel bar of D13 welded to the upper end plate. The hoop size is D6, with spacing of 150 mm.

Specimen test conditions are shown in Table 1. The experimental parameters were the shear span ratio (L/D = 3, 2), the axial load ratio, and the tip displacement of the columns at the initial loading. Two levels were set for the maximum tip displacement in each shear span ratio: for a shear span ratio of two, 1) displacement corresponding to the peak strength and 2) displacement where the lateral load drops to the yield strength after the peak; for a shear span ratio of three, 1) displacement where shear cracks are observed for plus and minus loading, and 2) displacement where compressive failure occurs.

2.3 Material properties

Standard tensile and compressive tests were conducted for the steel, concrete, polymer cement mortar, and epoxy resin that were injected into cracks of the damaged portions, to gain the mechanical proportion of the materials used. The measured results are present in Tables 1 and 2. Examples of the compressive stress–strain relations of epoxy resin are shown in Figure 3. It is apparent that the epoxy resin remains almost elastic until its compressive strength was twice the strength of concrete. Its strain was about 0.015.

Table 2 – Material properties of the steels used

			Young's Modulus ${}_sE$ ($\times 10^3$ N/mm^2)	Yield strength σ_Y (N/mm^2)	Yield strain ε_Y	Tensile strength σ_U (N/mm^2)	Yield Ratio σ_Y/σ_U	Elongation (%)
Steel	Chord	B3 Series	201	354	0.00176	473	0.748	31.5
		B2 Series	206	355	0.00170	479	0.742	33.1
	Batten plate		212	382	0.00180	520	0.735	26.4
Reinforce ment	Main rebar D13	B3 Series	183	355	0.00194	496	0.715	23.6
		B2 Series	179	364	0.00203	513	0.710	19.3
	Hoop ϕ6	B3 Series	189	391	0.00206	515	0.758	25.7
		B2 Series	179	400	0.00224	518	0.773	20.3

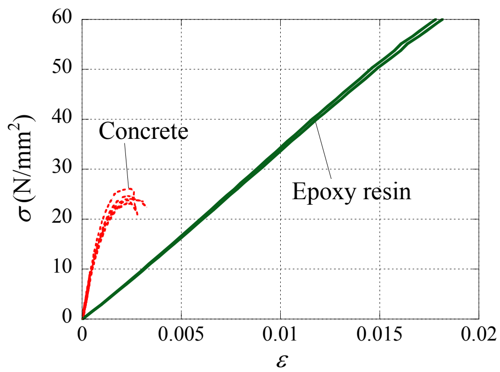

Fig. 3 – Stress–strain relation of epoxy resin.

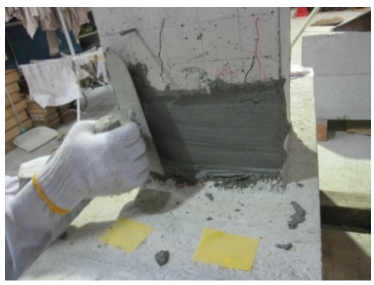

(a) Rebuilding of damaged cross section with PCM

(b) Injection of epoxy resin

Photo 1 – Method of retrofitting.

2.4 Method of retrofitting

The main retrofitting method includes the injection of epoxy resin into the observed cracks. The cross sections were rebuilt using polymer cement mortar (see Picture 1) before injecting the epoxy resin because the damage was heavy and the cover concrete was partially exfoliated. After removing the fragile portion of concrete, the primary resin was coated onto the surface to improve adhesiveness with the existing concrete. Then the section was rebuilt with polymer cement mortar.

Injection of the epoxy resin into cracks was conducted using the internal pressure of the rubber tube swollen by resin for injection. After removing surface dust, rubber tube attachments were put on the cracks with large width or the point where two cracks were crossed. The other cracked portions were caulked. Then rubber tubes were set and epoxy resin was injected. The surface was ground after the resin hardened.

3. Experimental results

3.1 Horizontal load–drift ratio relation

Figures 4 and 5 portray relations of horizontal load–drift ratio relations. The measured behaviors are shown as red and blue solid lines. Blue circles show the points at where the main reinforcement began yielding. Green squares show points at which the steel portion began yielding. The dotted line is the mechanism line, as obtained by assuming that a plastic hinge is formed at the bottom of the beam-column. Table 3 shows some part of the experimentally obtained results.

From these figures and table, it is apparent that initial stiffness of the retrofitted columns was lower than the initial columns, although the displacements experienced in each column differed. The value of the stiffness reduction ratio of $L/D = 2$ was larger than that of $L/D = 3$. The degradation amount of stiffness in second loading was small in case of $L/D = 2$. The stiffness of the retrofitted column decreases as the displacement in the first loading becomes larger. The lower stiffness might be attributed to deterioration of concrete rigidity, low rigidity of the resin and the polymer cement mortar, and imperfect injection of the resin.

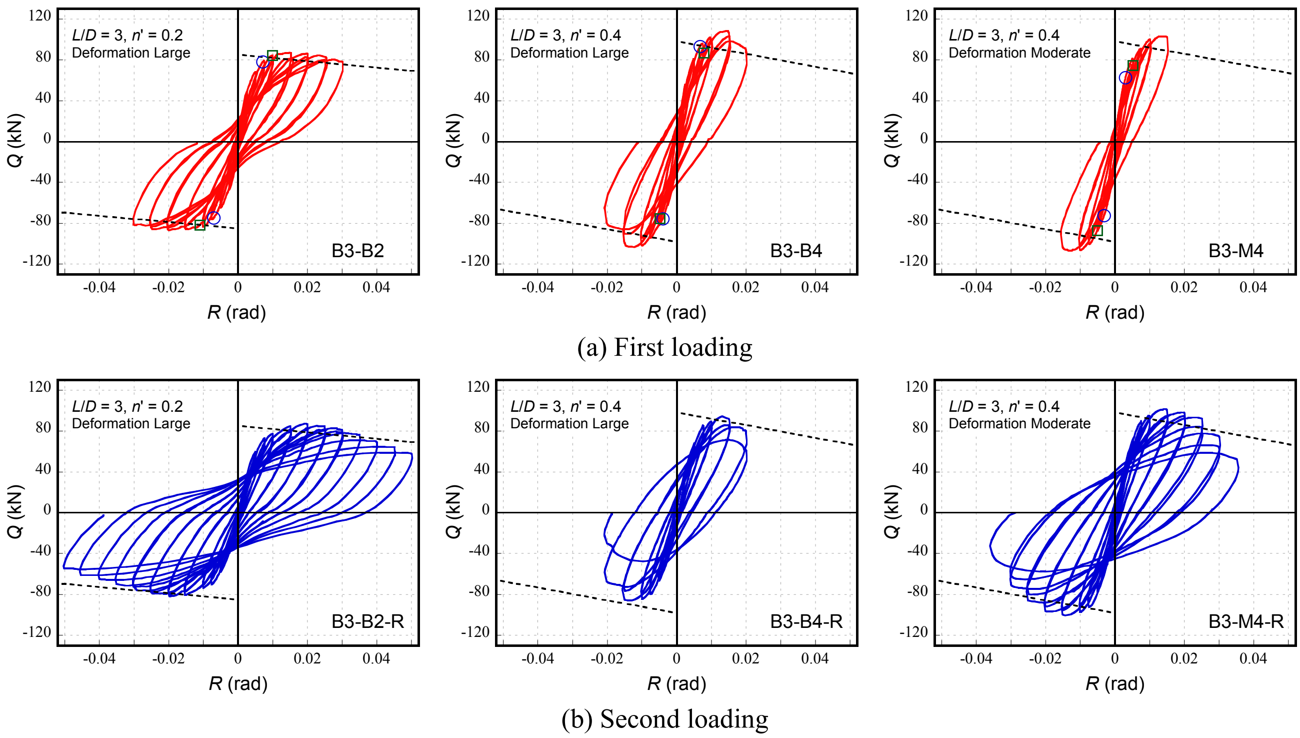

Fig. 4 – Relation between horizontal load–drift ratio ($L/D = 3$).

Experimental results also show that the column which experienced the larger displacement and higher axial load (Specimen B3-B4-R) showed lower load carrying capacity, but the others showed approximately equal capacities to those of the initial columns in the case of $L/D = 3$. In the case of $L/D = 2$, the maximum strength in the second loading became greater as the displacement in the first loading became larger. All retrofitted columns showed higher load-bearing capacity, even though the experienced displacements in each column differed. The lower load carrying capacity of the Specimen B3-B4-R resulted from buckling of longitudinal reinforcements. The higher load carrying capacity can be attributed to the effect of strain aging and strain hardening of the steels.

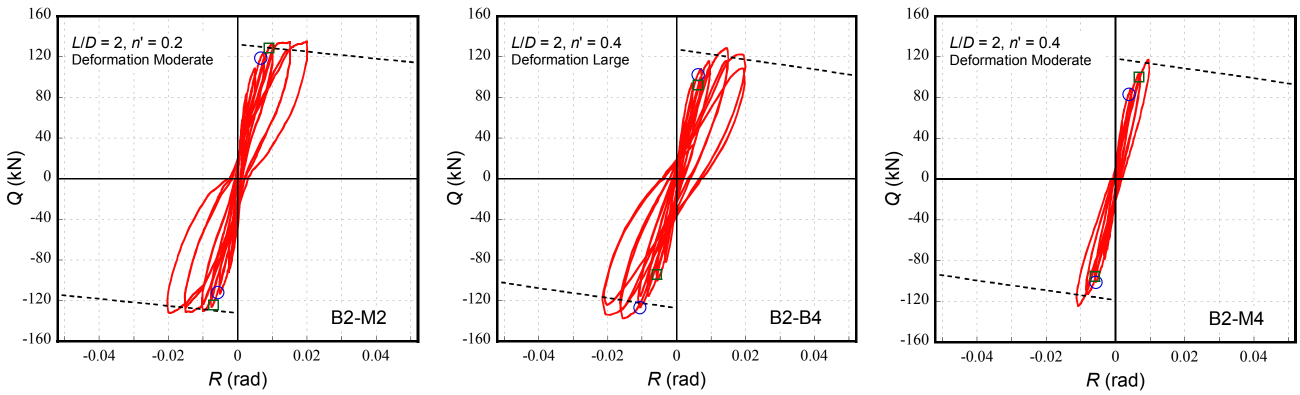

(a) First loading

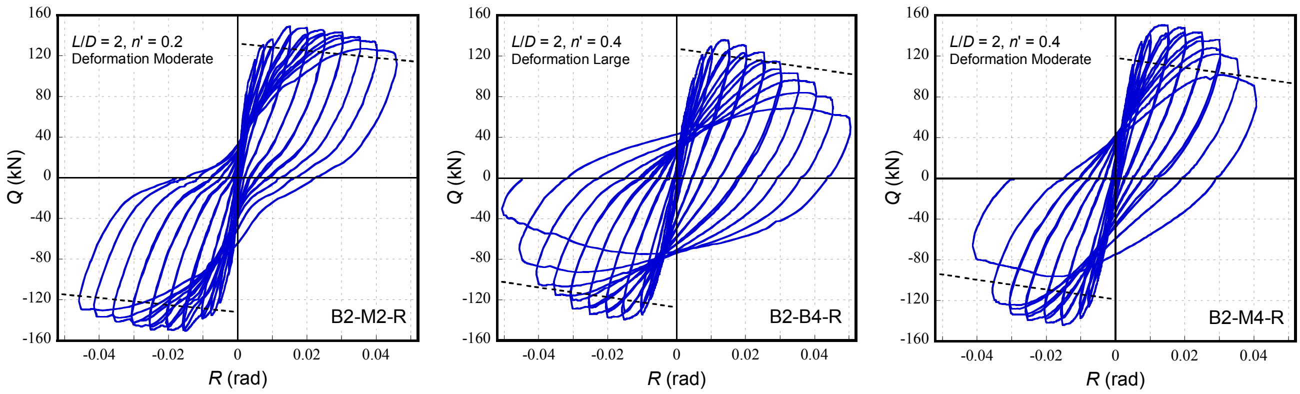

(b) Second loading

Fig. 5 – Relation between horizontal load–drift ratio ($L/D = 2$).

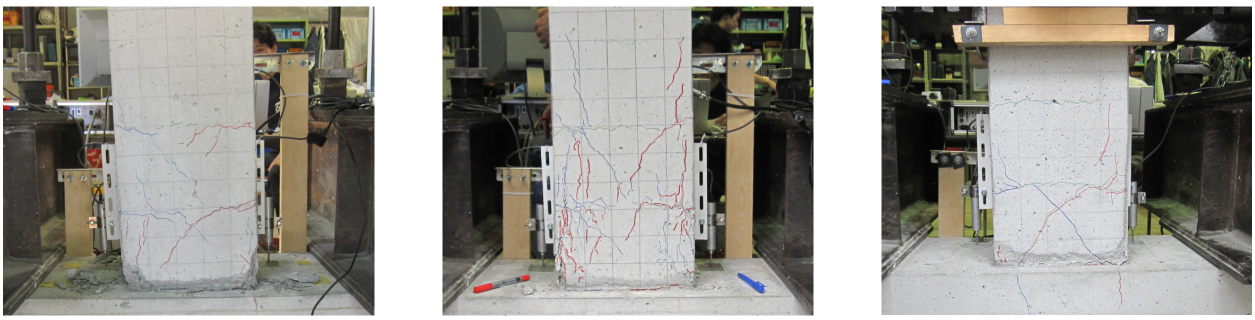

(a) B3-B2 (R=0.03rad) (b) B3-B4 (R=0.02rad) (c) B2-M2 (R=0.02rad)

Photo 2 – Typical damage of specimens in first loading.

Table 3 – Experiment results

Specimens		Initial stiffness (kN/mm)	Stiffness reduction ratio (%)	Maximum Strength (kN)		Deformation angle at max. strength (rad.)	
						+	-
1st loading	B3-B2	32.9	-	86.9	-	(0.015)	(-0.020)
	B3-B4	34.4	-	105.9	-	0.015	-0.012
	B3-M4	37.2	-	104.8	-	0.014	-0.013
2nd Loading	B3-B2-R	24.4	74.2	84.5	0.97	0.020	-0.020
	B3-B4-R	24.6	71.4	90.2	0.85	0.013	-0.013
	B3-M4-R	31.8	85.5	100.9	0.96	0.014	-0.014
1st loading	B2-M2	102.7	-	133.4	-	(0.020)	(-0.020)
	B2-B4	67.3	-	133.0	-	0.145	-0.015
	B2-M4	66.2	-	120.9	-	-	-
2nd Loading	B2-M2-R	100.4	97.8	149.7	1.12	0.015	-0.015
	B2-B4-R	64.8	96.3	137.4	1.03	0.014	-0.015
	B2-M4-R	62.7	94.7	147.2	1.22	0.013	-0.015

3.2 Width of flexural cracks

Flexural crack widths were measured to elucidate the relation of crack width and the experienced drift ratio. These are valuable to predict the degree of damage from the crack width after an earthquake. Figure 6 shows the relation between maximum widths of the crack–drift ratio.

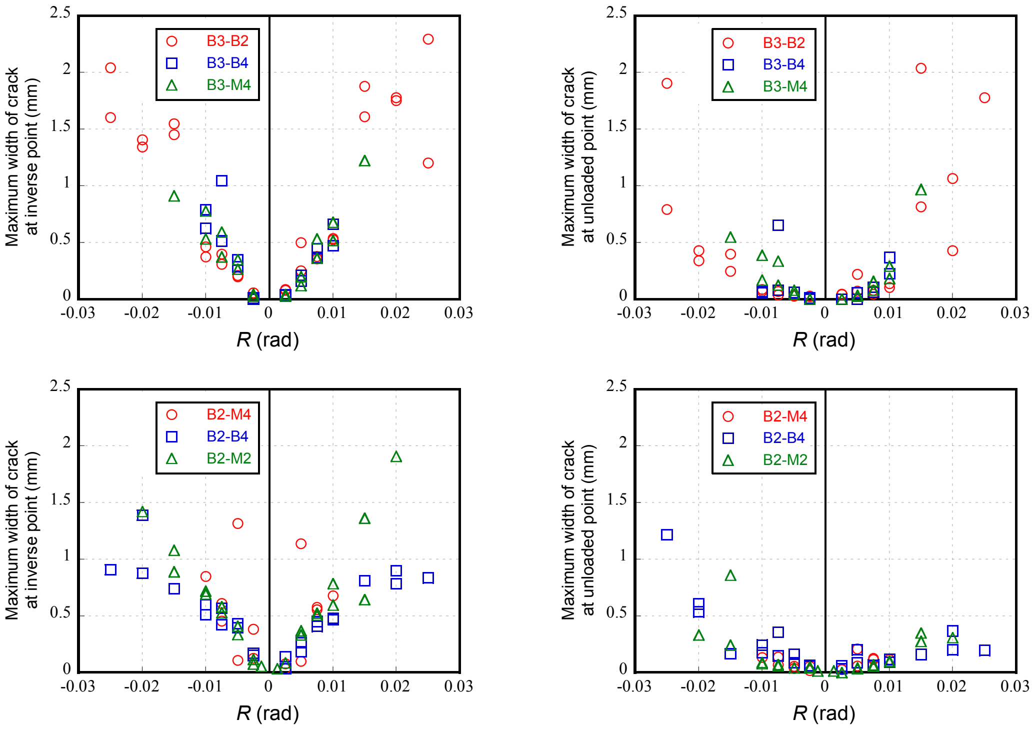

Fig. 6 – Relation between maximum width and the crack–drift ratio.

The relation between maximum widths of a crack at an inverse point and the drift ratio were approximated as a linear relation. However, it is impossible to measure or estimate the maximum widths of cracks after an earthquake. Maximum widths of a crack at an unloaded point were not linear to the drift ratio because of the effect of displacement by elastic unloading. It is difficult to estimate the damage to a beam-column from this. However, a sudden change in these relations is apparent after 0.01 rad, which presents the possibility of beam-column damage estimation.

4. Evaluation of structural performance

4.1 Analytical method

Numerical analysis was conducted to explain the behavior of the retrofitted columns. The bending moment versus the curvature relation was calculated using the so-called finite fiber method. The following assumptions were adopted: 1) the plane section remains planar after bending, 2) tensile strength of concrete is ignored, 3) shear deformation is ignored, and 4) the rotation angle of the beam-column is concentrated within the plastic hinge region. The Sakino–Sun stress-strain relation was used for concrete [Sakino and Sun 1994]. The bilinear model and Kato's cyclic stress–strain curve were used for the steel and reinforcing bar [Kato et al. 1973]. The strain hardening coefficient was set as 0.005. The plastic hinge length was determined using Sakai's model [Sakai and Matsui 2000].

Figure 7 shows the stress–strain relation of concrete in the second loading. It is a hysteresis after the last hysteresis during the first loading. The last unloaded point in the first loading is taken as the origin for the hysteresis curve of concrete under the second loading. The hysteresis rule is also moved to the new origin. Furthermore, stress during the second loading is assumed to be less than the skeleton curve of the first loading.

Regarding a damaged and retrofitted specimen, the possibility exists that the yield stress of the yielded steel becomes higher than the initial one because of strain aging and strain hardening. Herein, these effects are considered and analyzed. The yield stress as 1.2 times the initial yield stress [Fujinaga and Sun 2012]. The yield stresses of the steel and steel bar are thereby increased at the same rate.

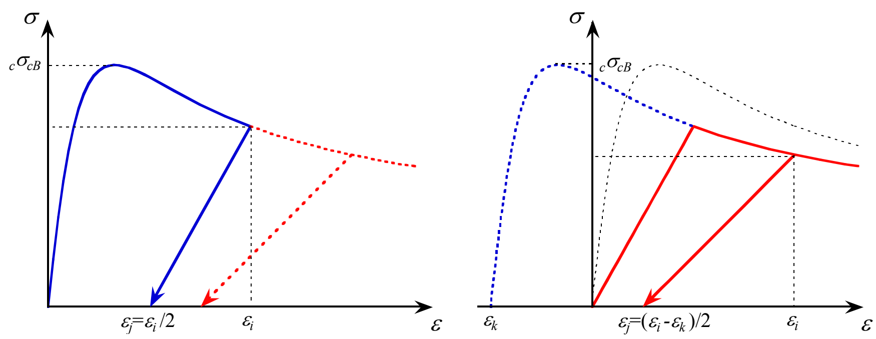

(a) First loading (b) Second loading

Fig. 7 – Stress–strain relation of concrete.

4.2 Comparison with the experimentally obtained results

Figures 8 and 9 present a comparison of analytical and experimental behaviors. Dotted lines show the experimentally obtained results. Red and blue solid lines show analytical results. Analytical results predicted the stiffness reduction ratio and the experimental behaviors fairly well. However, in the case of retrofitted beam-columns, the analytical results underestimate the experimental behavior, probably because of the effect of strain aging and strain hardening of steel.

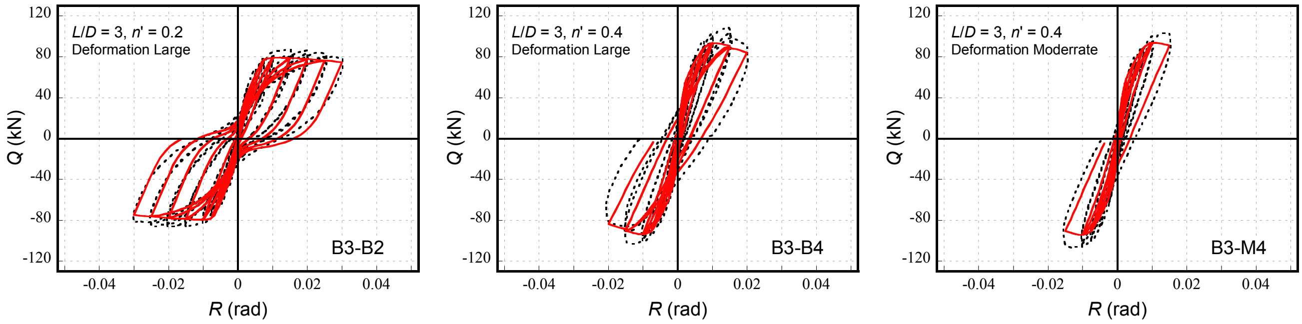

(a) First loading

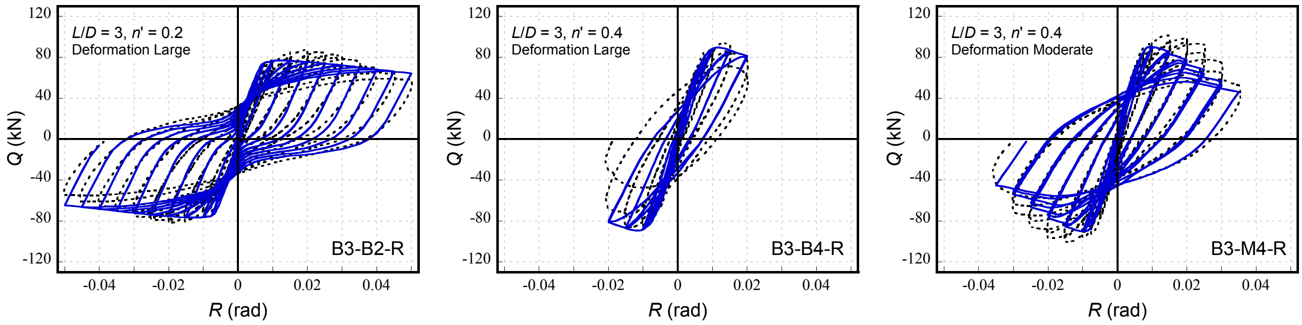

(b) Second loading

Fig. 8 – Analytically and experimentally obtained results ($L/D=3$).

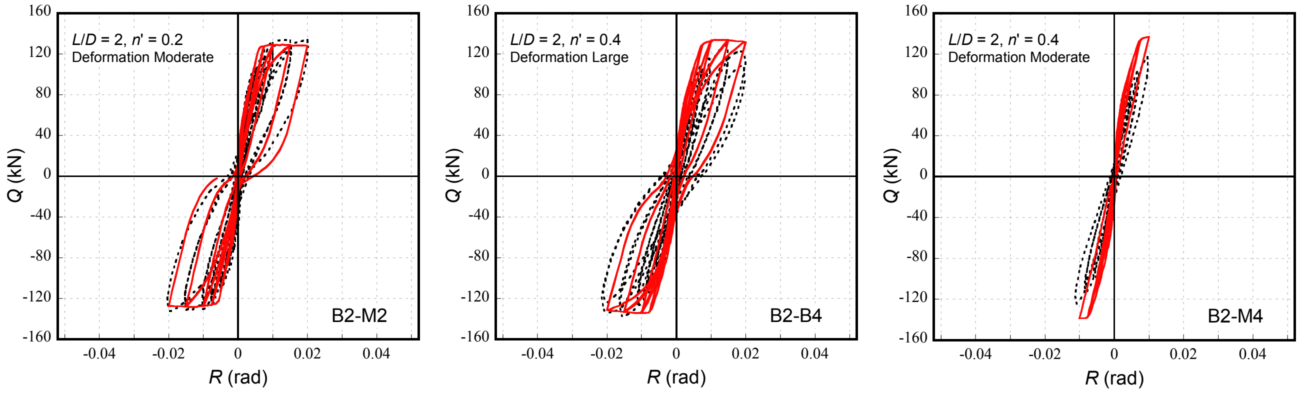

(a) First loading

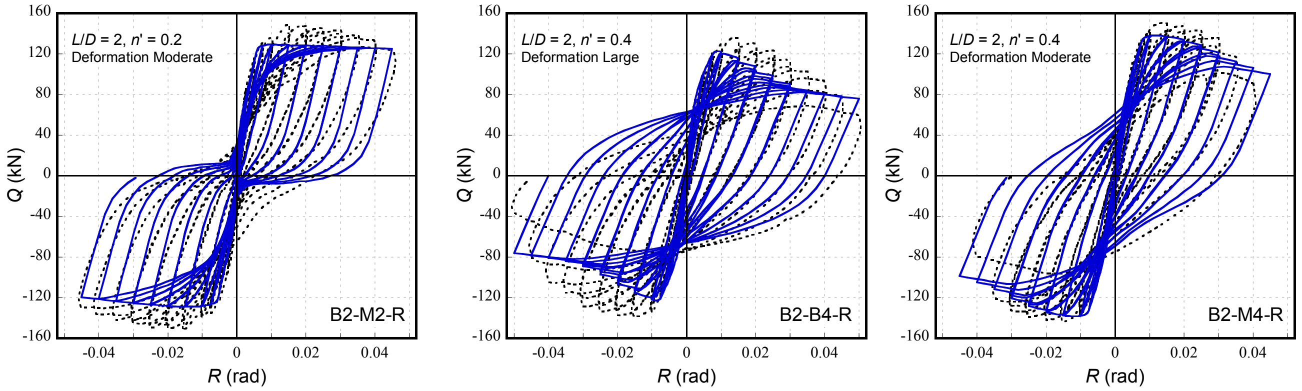

(b) Second loading

Fig. 9 – Analytically and experimentally obtained results ($L/D=2$).

Table 4 and Figure 10 show a comparison of behavior that incorporates an increment of 20% of the steel yield stress. The analytical results can predict the measured ones much better in terms of their load-carrying capacities and post-peak behaviors in comparison with the results, which do not consider the increase of yield stress.

Table 4 – Analytical results

Specimens	Stiffness decline ratio		Strength prediction ratio							
			$1.0\,\sigma_Y$				$1.2\,\sigma_Y$			
	Experiment	Analysis	maximum	0.005 rad	0.01 rad	0.02 rad	maximum	0.005 rad	0.01 rad	0.02 rad
B3-B2-R	0.742	0.765	0.907	1.027	0.960	0.951	1.002	1.019	1.111	1.055
B3-B4-R	0.714	0.617	0.991	0.933	1.215	1.122	1.073	0.933	1.068	1.240
B3-M4-R	0.855	0.669	0.894	0.906	0.931	0.796	0.959	0.906	1.071	0.887
B2-M2-R	0.978	0.959	0.863	0.938	0.871	0.869	0.949	0.938	1.028	0.956
B2-B4-R	0.963	0.860	0.894	1.082	0.916	0.804	0.967	1.082	1.008	0.905
B2-M4-R	0.947	0.877	0.940	0.980	0.991	0.963	1.024	0.980	1.065	1.056

The analytical results considering above described assumptions that predicted the experimental behaviors well, which implies the validity of the analytical method presented in this paper for evaluation of the structural performance of retrofitted SRC columns. The last loop behavior cannot be predicted using the modified method, probably because of handling of the buckled reinforcing bar. Buckling of the main reinforcements is ignored in this analysis.

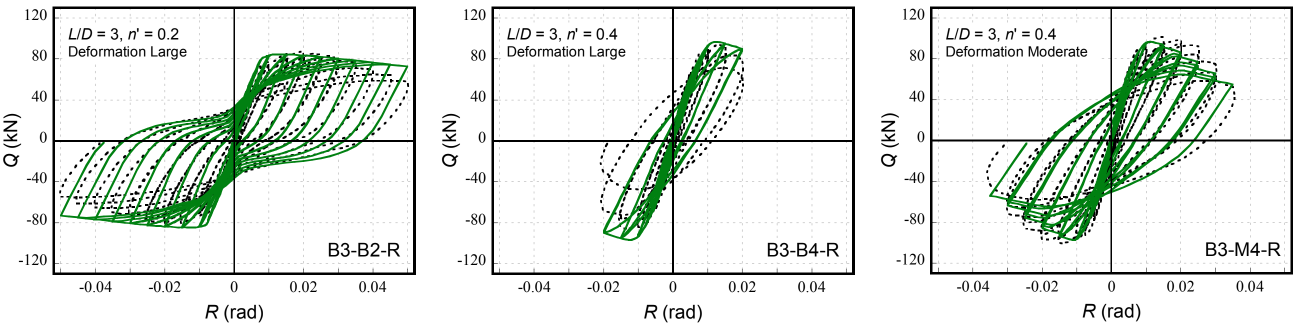

(a) B3 Series ($L/D = 3$)

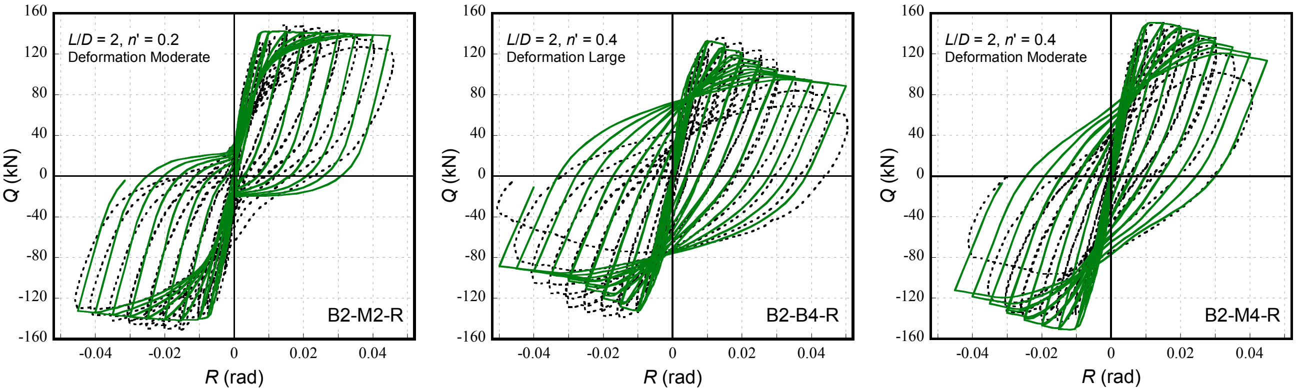

(b) B2 Series ($L/D = 2$)

Fig. 10 – Comparison of analytically and experimentally obtained results ($1.2\,{}_s\sigma_Y$).

5. Conclusions

From experimental and analytical results obtained for six open-web type SRC beam-columns with bolt-connected batten steel plates described in this paper, the following inferences can be drawn.

(1) Initial stiffness of the retrofitted columns was lower than the initial ones. The value of stiffness reduction ratio of $L/D = 2$ was found to be larger than that of $L/D = 3$. The lower stiffness might be attributed to deterioration of concrete rigidity, low rigidity of the resin, and the polymer cement mortar, in addition to imperfect injection of the resin.

(2) The retrofitted columns showed approximately equal capacities to those of the initial columns in the case of $L/D = 3$. In the case of $L/D = 2$, the maximum strength in the second loading becomes larger. The higher load carrying capacity can be attributed to the effect of strain aging and strain hardening of the steels. The effect of buckling of longitudinal reinforcements was observed in the column which experienced the larger displacement and higher axial load.

(3) Analytical results predicted the stiffness reduction ratio and the experimental behaviors fairly well. However, for retrofitted beam-columns, the analytical results underestimate the experimental behavior.

(4) Analytical results considering the increment of 20% of the yield stress of the steel predicted the experimental behaviors well, which implies the validity of the analytical method presented in this paper for the evaluation of the structural performance of retrofitted SRC columns.

Acknowledgements

This work was supported by JSPS KAKENHI Grant-in-Aid for Scientific Research (C) Number 25420579. We would like to express our gratitude to Mr. Kume, who cooperated with this experiment and analysis.

References

[1] Editorial Committee for the Report on the Hanshin-Awaji Earthquake Disaster (1998). Report on the Hanshin-Awaji Earthquake Disaster, AIJ.

[2] Sakino K, Sun Y (1994): Stress–Strain Curve of Concrete Confined by Rectilinear Hoop. *J. Struct. Constr. Eng., AIJ*, **461**, 95-04.

[3] Kato B, Akiyama H, Yamauchi Y (1973): Cyclic stress–strain relations for steel based on experimentally obtained results, *Summaries of Technical Papers of Annual Meeting*, *AIJ*, 937-938.

[4] Sakai J, Matsui C (2000): Hysteresis Characteristic of Steel Reinforced Concrete Beam-Columns. *J. Struct. Constr. Eng.*, *AIJ*, **534**, 183-190.

[5] Fujinaga T, Sun Y (2012): Structural Performance of Damaged Open-web Type SRC Beam-columns after Retrofitting. *15th World Conference of Earthquake Engineering*, Lisbon, Portugal.